ADVANCED MATERIALS INTERFACES

www.advmatinterfaces.de

Annealing of Polyelectrolyte Multilayers for Control over Ion Permeation

*Dennis M. Reurink, Jord P. Haven, Iske Achterhuis, Saskia Lindhoud, (Erik) H. D. W. Roesink, and Wiebe M. de Vos**

Polyelectrolyte multilayer based membranes are highly promising systems to create stable and versatile nanofiltration membranes. One very popular and well-studied polyelectrolyte pair, is the polycation poly(diallyldimethylammonium chloride) (PDADMAC) and polyanion poly(sodium 4-styrenesulfonate) (PSS), due to its excellent separation properties and high chemical and physical stability. Membrane charge can be easily controlled by simply terminating the multilayer by either PDADMAC or PSS. Unfortunately, a phenomenon that occurs during multilayer coating, is overcompensation by PDADMAC. In this study, it is shown that overcompensation of PDADMAC results in a positive surface charge even when the multilayer is PSS-terminated. In addition, it is shown that this leads to poorer membrane separation properties with sulfate retention decreasing from 94 to 39%. At the same time, it is demonstrated that a so-called annealing cycle with a high salt concentration leads to recovery of the negative surface charge, increasing the sulfate retention from 39 to 95%. Even for multilayers at which no irreversible positive surface charge is measured, separation properties improved substantially (increasing sulfate retention from 94 to 97%, at a higher membrane permeability) after salt-annealing. It is concluded that post-treatment by salt-annealing results in an improved membrane performance and allows an additional degree of control over the membrane separation properties.

1. Introduction

In membrane filtration there are four types of membranes commonly used: microfiltration, ultrafiltration, nanofiltration, and (reverse or forward) osmosis membranes.[1] Micro- and ultrafiltration are pore-flow membranes and separation is based on their porous structures where reverse osmosis (RO) membranes are based on dense separating layers and separation takes place by means of solution-diffusion.[2] Nanofiltration (NF) membranes fall in the transition region between pore-flow and solution-diffusion membranes and typically have a dense separating layer which is more open than an RO membrane.[2] This dense separating layer—in both RO and NF membranes—is usually a thin film prepared by interfacial polymerization (IP). These membranes are termed thin film composite membranes because of their selective top layer and porous support for mechanical strength, and are commercially widely available.[3] However, commercial RO and NF membranes are mostly based on a flat sheet configuration. To obtain a higher surface-to-volume ratio, hollow fiber membranes are of more interest. However, these are notoriously difficult to coat by IP.[4]

One recent breakthrough in membrane material science is an alternative to IP that allows coating of thin polymeric films (<50 nm) on a surface independent of its geometry. This versatile technique is termed layer-by-layer (LbL) assembly of polyelectrolytes,[5] in which two oppositely charged polyelectrolytes are coated alternately on a charged surface to create polyelectrolyte multilayers (PEMs).[6] The choice of polyelectrolyte pairs,[7] salt concentration,[8] and pH[9] are of great importance for the properties of the thin film. PEMs can be formed via several approaches including immersive, spin, spray, electromagnetic, and fluidic methods that each have their own advantages and disadvantages.[10] This breakthrough has led to an increasing interest in PEM-based membranes for both NF and RO applications.[11,12] Various charged support surfaces such as poly(ethersulfone),[13] sulfonated poly(ethersulfone),[14] polysulfone,[15] plasma-treated poly(acrylonitrile)/poly(ethylene terephthalate),[16] and porous alumina supports[17] have been investigated. In most cases a tight ultrafiltration support membrane is used to quickly obtain a separation layer that has nanofiltration properties and a good coverage of the surface. Although several modified membranes have been studied based on various polyelectrolytes, special interest has been shown in PEM

D. M. Reurink, J. P. Haven, I. Achterhuis, Prof. (E.) H. D. W. Roesink, Dr. W. M. de Vos
Membrane Science and Technology
University of Twente
MESA+ Institute for Nanotechnology
P.O. Box 217, 7500 AE Enschede, The Netherlands
E-mail: w.m.devos@utwente.nl

Dr. S. Lindhoud
Nanobiophysics
University of Twente
MESA+ Institute for Nanotechnology
P.O. Box 217, 7500 AE Enschede, The Netherlands

DOI: 10.1002/admi.201800651

membranes based on poly(diallyldimethylammonium chloride) (PDADMAC) and poly(sodium 4-styrenesulfonate) (PSS). This polyelectrolyte couple has been well studied for its anion selectivity toward fluoride,[18] sulfate,[19] and phosphate[20] and outperforms most commercial membranes in terms of the combination of permeability and selectivity. Since most commercial nanofiltration membranes consist of a thin polyamide film, they are prone to degradation once the membrane is cleaned with hypochlorite.[14] PSS/PDADMAC membranes show superior chemical stability toward hypochlorite up to a hundred times higher in comparison with commercial polyamide-based membranes.[14]

In the formation of PEMs, increasing the salt concentration results in thicker PEMs at an equal number of layers.[21,22] When a PEM is coated on top of a membrane, the pores of the membrane must first be closed until a defect-free separating layer can be formed. Two distinct regimes can be defined here: the pore-dominating regime and the layer-dominating regime.[22] When the salt concentration is increased, the layer-dominated regime is reached with fewer coating steps. From a manufacturing perspective it would be beneficial to coat PEMs at high salt concentrations in order to make the procedure less labor intensive. Unfortunately, a phenomenon that occurs when a PSS/PDADMAC multilayer becomes too thick is overcompensation of PDADMAC, thereby creating an excess of positive charge in the multilayer.[23] This phenomena has been mainly observed at high salt concentrations, since thick layers are easily obtained at such high ionic strengths.[17,22] In these studies, zeta potential measurements have shown that the multilayer becomes positive after a certain number of layers when coated at high ionic strengths. An excess of positive charge is expected to be undesirable for PEM-coated membranes for several reasons: excess charge will induce more swelling[24] and, in turn, lead to a more open and less selective layer. Moreover, positively charged layers tend to be more susceptible to fouling.[25]

A method to counteract the excess of positive charge was proposed by Fares et al.[26] who annealed PSS/PDADMAC multilayers with a 2 M NaCl salt solution. They showed that when PSS/PDADMAC multilayers are exposed to 2 M salt concentration, excess PDADMAC evenly disperses throughout the multilayer. This method is effective because PSS/PDADMAC multilayers undergo a glass transition for NaCl concentrations higher than 1.5 M or temperatures higher than 45 °C.[27] Under these conditions, the excess of PDADMAC will reach the surface and for that reason will be able to take up PSS until the surface is saturated. Subsequently, multiple annealing cycles were performed to obtain a stoichiometric multilayer, which was reached after six annealing cycles.

In this work, for the first time, we show that salt-annealing of PSS/PDADMAC multilayers can be used to prepare PEM-coated membranes with excellent separation properties. We systematically study the buildup of positive charge in PSS/PDADMAC multilayer and the negative impact this has on membrane performance. Moreover, we show that membrane performance can be recovered by annealing the PEM-based membranes. To do this, PSS/PDADMAC multilayers are coated on hollow fiber membranes in a 1.0 M NaCl solution. The membrane performance is tested on the retention of mono- and divalent salts: NaCl, Na_2SO_4, and $MgCl_2$. To characterize the surface of the membrane, zeta potential and contact angle measurements are performed after each coated monolayer. These measurements allow us to understand why the membrane performance changes after each coating step and annealing cycle. Finally, we will show that the membrane becomes positively charged after a certain number of layers and that this affects the performance of the membrane. Through annealing, the charge can be reversed and we study the effect of the number of annealing cycles on the performance of the membrane.

2. Results and Discussion

In this section, we will initially focus on the characterization of the PSS/PDADMAC multilayer prepared at an ionic strength of 1.0 M of NaCl by means of reflectometry, zeta potential, and contact angle measurements. Here, it is shown that the multilayer is successfully grown on porous hollow fiber supports and that the surface properties change as function of the multilayer thickness. In order to understand the change in surface properties, the PEMs are, in the second part, assessed for their ion rejection performance. We subsequently correlate the characterization results obtained in the first part to the ion rejection behavior obtained in the second part. This correlation provides an improved understanding of the ion rejection properties of the PSS/PDADMAC PEM as a function of the number of layers on the surface.

2.1. Polyelectrolyte Multilayer Characterization

Applying optical fixed angle reflectometry, the growth of PSS/PDADMAC multilayers at an ionic strength of 1.0 M NaCl on a silicon wafer was studied. Here, two polyelectrolyte solutions are alternately flown through the fluid cell where adsorption to a silicon wafer is measured. After each polyelectrolyte deposition, the cell was flushed with a solution containing the same ionic strength as the polyelectrolyte solution in order to prevent the formation of PDADMAC and PSS complexes. The point of measurement occurs at a stagnant point under well-defined hydrodynamic conditions on the silicon wafer. This means that at this point no shear is applied and adsorption only takes place based on diffusion. This is important since shear can influence the buildup of a PEM.[28] When measuring at the stagnant point within the cell, the multilayer is formed via electrostatic interactions and a typical growth profile is obtained as shown in **Figure 1** with the adsorption on the left axis. This figure shows the nonlinear-to-linear growth of PSS and PDADMAC under an ionic strength of 1.0 M of NaCl as was also shown by Dubas and Schlenoff,[8] and McAloney et al.[21] The dry layer thickness on the right axis in Figure 1 is calculated by dividing the adsorption data by the density of a PSS/PDADMAC multilayer of 1.07 g cm^{-3}.[29] In addition, dry layer thickness of the multilayer (shown in Figure 1 by the red dots) was measured by ellipsometry; resulting in a thickness of a 9, 13, and 17 thick layers being 32 ± 0.5, 67 ± 2.8, and 97 ± 2.2 nm, respectively, further indicating a linear growth at thicker layers. The calculated and measured thicknesses are for dry layers, when these layers are immersed in water the thickness will increase due to swelling of the layers by 30 to 40%.[29]

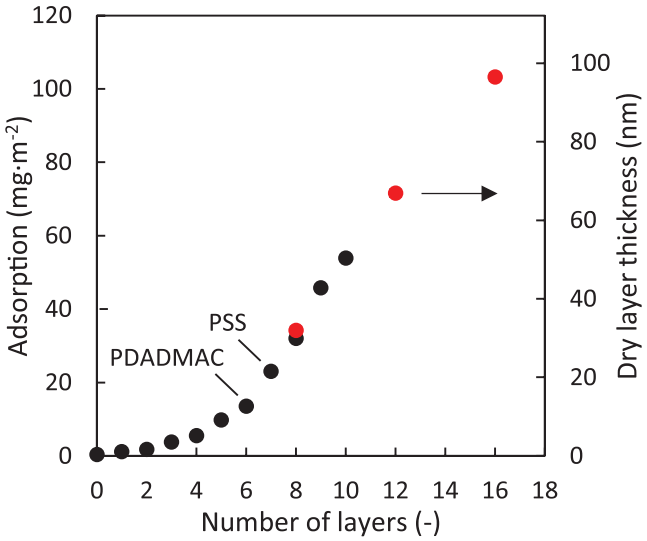

Figure 1. Multilayer growth measured using reflectometry and ellipsometry. On the left axis: adsorption (mg m^{-2}) of PSS (odd) and PDADMAC (even) at an ionic strength of 1.0 M NaCl on a silicon wafer is plotted as function of the number of layers to form a PEM. On the right axis: dry layer thickness (nm) of the PSS/PDADMAC multilayer as function of the number of layers. The dry layer thickness is calculated by using a PSS/PDADMAC multilayer density of 1.07 g cm^{-3} (black dots). Indicated by the arrow and red dots are the dry layer thicknesses of the PSS/PDADMAC multilayer measured by ellipsometry.

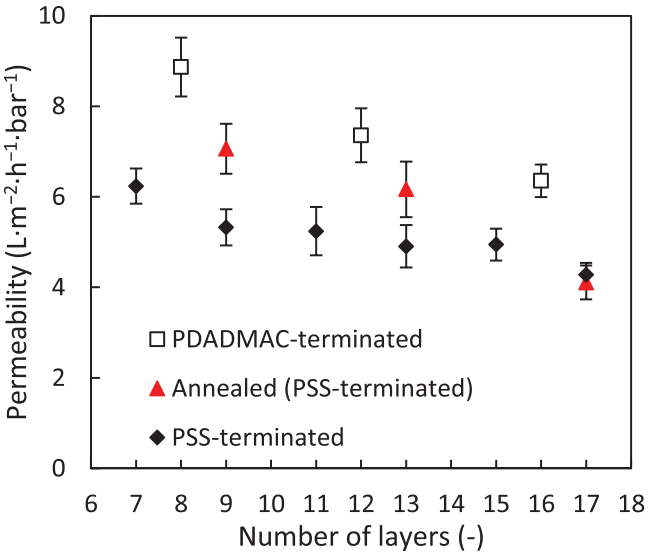

Figure 2. Permeability (L m^{-2} h^{-1} bar^{-1}) as function of the number of layers for a PSS/PDADMAC multilayer coated hollow fiber membrane prepared at 1.0 M of NaCl. The nonannealed multilayer is either terminated by PDADMAC, indicated by open squares, or PSS, indicated by black diamonds. Annealed PSS-terminated multilayers are indicated by red triangles.

The PSS/PDADMAC multilayers were also coated on porous hollow fiber support membranes by dip-coating the supports alternately in the corresponding polyelectrolyte solutions. After each coating step the multilayer is rinsed with a solution containing the same ionic strength as the polyelectrolyte solutions. In dip-coating, adsorption of polyelectrolytes is based on diffusion just like in the reflectometry measurements. Therefore, the two coating procedures will lead to highly comparable PEM-coatings.

When coating the multilayer on a porous membrane support it is important to make sure that the multilayer covers all the pores. From literature it is known that a zig-zag behavior is observed in the permeability of the membrane when coating PSS and PDADMAC alternately.[22] This behavior is termed the odd-even effect and it occurs when two polyelectrolytes are alternatingly deposited on a surface.[30] This odd–even effect is also observed in membrane permeability measurements and is due to the difference in swelling of PDADMAC-terminated multilayers compared to PSS-terminated multilayers; where PDADMAC-terminated multilayers show a swelling that is much higher than for PSS-terminated multilayers.[31] When PEMs are coated on porous membrane supports, a pore-dominated and a layer-dominated regime can be found.[22] In the pore dominated regime, a PDADMAC-terminated membrane shows a higher resistance than a PSS-terminated membrane, because the higher swelling of PDADMAC results in pore closure; an effective decrease in pore diameter. In the layer dominated regime, however, the higher swelling of PDADMAC gives a lower resistance, and therefore a higher permeability, because the entire multilayer becomes less dense. It is important to be in the layer dominated regime to ensure a defect free layer. In **Figure 2**, the permeability of the membrane is plotted as function of the number of layers. Here, it can be seen that the coated PEM membrane has a permeability of around 4–10 L m^{-2} h^{-1} bar^{-1}, which is a typical value for NF membranes. A PSS-terminated multilayer has a lower permeability than a PDADMAC-terminated multilayer indicating the layer dominated regime. This means that the membrane is completely covered by the PEM and that the permeability and separation properties will be fully determined by the PEM.

To anneal the multilayer, the multilayer is immersed in a solution containing a high ionic strength of 2.0 M of NaCl which results in an increased mobility of the polyelectrolytes within the multilayer.[26] Afterward, the membranes are dip-coated in the PSS polyelectrolyte solution at an ionic strength of 1.0 M of NaCl. The immersion and dip-coating is considered as one annealing cycle; in total, six annealing cycles are applied to create an annealed multilayer. In a similar procedure described by Fares et al.[26] In that work, it was shown using radioactive labeled counter ions that with each annealing cycle more PSS is adsorbed. Figure 2 shows that the permeability of the annealed membrane is higher compared to a nonannealed multilayer. This can be explained by the adsorption of more negative charges in the multilayer which leads to a higher degree of swelling, and supports the work of Fares et al.[26]

The zeta potential of the PEM-coated membranes was measured by means of streaming potential using hollow fiber membranes. Numerous studies have shown streaming potential measurements to be a viable method[32–35] and it is commonly used in a hollow fiber configuration.[14,22,36] Every layer of the membrane was prepared separately to give the most accurate result of the zeta potential, because the shear stresses accompanied with streaming potential measurements can influence the properties of the multilayer.[37] In this study, care was taken to

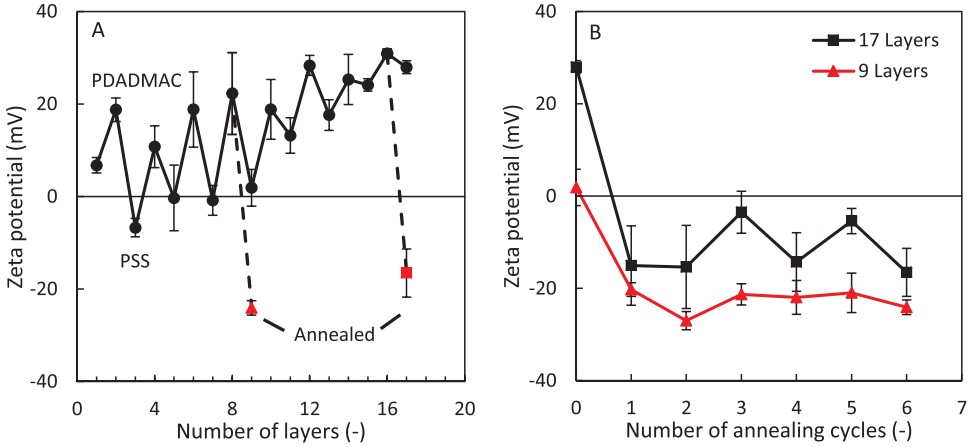

Figure 3. A) Zeta potential of a PSS/PDADMAC PEM prepared at an ionic strength of 1.0 M NaCl as function of the number of layers. The PEM was coated on a hollow fiber support membrane. The solid line represents the normal PEM buildup, the dashed lines and the red triangles represent an annealed PEM. B) Zeta potential as function of the number of annealing cycles for a PEM-coated hollow fiber membrane. The black solid line represents a multilayer of 17 layers thick and the red solid line represents a multilayer of nine layers thick.

produce every module in an identical fashion and various modules were measured in order to obtain a reliable result.

In **Figure 3**A, the typical zig-zag pattern is obtained that has been observed for many PEMs,[7,17,38] showing that the surface charge is positive after adsorption of the polycation and negative after polyanion adsorption. Already after the fourth layer, the zeta potential was positive when terminated with PDADMAC or neutral when terminated with PSS. This trend continues until the ninth layer. After the ninth layer, the zeta potential shifts to positive potentials. The potential of the multilayer stays positive even though the multilayer is terminated with the negatively charged PSS. This was also reported by Adusumilli and Bruening[17] and de Grooth et al.[22] for PEM-coated membranes prepared at ionic strengths of 1.0 and 0.5 M of NaCl, respectively. This is most likely due to the buildup of PDADMAC in the PEM bulk, as described by Ghostine et al.[23] and Fares et al.,[26] Kelly et al.[39] In these works, an increasing amount of PDADMAC was observed throughout the multilayer for thicker multilayers. Arias et al.[40] showed even that excess PDADMAC, in a PSS-terminated multilayer, diffuses up to the surface over time when stored in saline water (0.15 M NaCl). In the present study, we show that a PSS/PDADMAC multilayer grown at an ionic strength of 1.0 M NaCl on a membrane surface, shows the same trend in the zeta potential measurements as the above mentioned studies. The measurements show, that the surface properties are greatly influenced by the buildup of PDADMAC within the multilayer.

Annealing of the polyelectrolyte multilayer membranes was performed in 6 cycles using the procedure described earlier. In Figure 3A, as indicated by the dashed line, a 9- and 17-layer thick annealed multilayer had a negative zeta potential and not a positive zeta potential of a nonannealed PSS-terminated PEM. To investigate if the number of annealing cycles influenced the streaming potential, various membranes were measured for varying number of annealing cycles; as shown in Figure 3B. Here, it can be seen that for both a 9 and 17 layer thick PEM, the streaming potential reached its most negative value after the first annealing cycle. This means that the surface charge properties of the multilayer are not influenced by the number of annealing cycles, most likely due to the relatively thin multilayers used in this study in comparison to others[26] and the long annealing times used in this study.[41]

The effect of annealing was also studied by contact angle measurements. Taking the captive bubble approach is essential here as it ensures that the multilayer is in its hydrated state and the contact angle measured is more accurate. From literature it is known that the contact angle of a multilayer is dependent on the terminating layer, creating a zig-zag pattern, and that a PDADMAC-terminated multilayer has a 10°–40° higher contact angle than a PSS-terminated multilayer.[42–44] In **Figure 4**, the results of the contact angle measurements are presented and it is observed that a PDADMAC-terminated layer (eighth layer) has a 25° higher contact angle than a PSS-terminated layer (ninth layer). However, the difference between the contact angle of the 12th and 13th layer is already smaller than 10°. Furthermore, no significant difference in the contact angle is observed between the 16th and 17th layer. This means that the zig-zag pattern disappeared and that the terminating layer is no longer influencing the multilayer properties. In addition, the contact angle of a PSS-terminated multilayer increases from 30° to 47°, comparing the 9th and the 17th thick layer, indicating a higher influence of PDADMAC. This result correlates well with the zeta potential results and is most likely due to the overcompensation of PDADMAC in the multilayer. Annealing of the multilayer shows that the contact angle decreases to a value of around 30°, for the 13th and 17th thick layer, indicating a higher influence of the surface from the PSS. This shows that annealing counteracts the overcompensation of PDADMAC as was also shown by the zeta potential results.

2.2. Salt Retention of Polyelectrolyte Modified Membranes

In the previous section, it was shown that the surface properties of thicker PSS/PDADMAC multilayers are dominated by PDADMAC, and that for thicker layers, the surface properties no longer depend on the terminating polyelectrolyte layer. It was also shown that annealing alters the surface properties

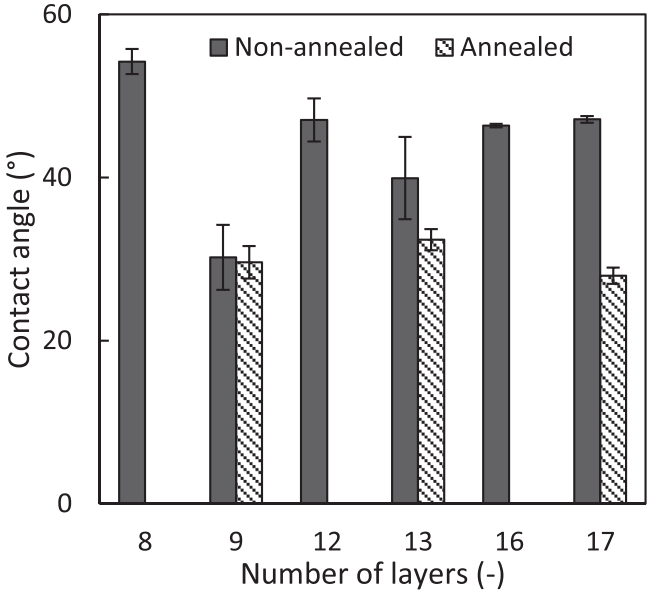

Figure 4. Captive bubble contact angle of a silicon wafer coated with a PSS/PDADMAC multilayer as function of the number of layers. Odd layers are PSS-terminated multilayers and even layers are PDADMAC-terminated multilayers. Solid bars represent the nonannealed membranes and patterned bars represent the annealed membranes. The silicon wafers were immersed in water coated-side-down and an air bubble was released on the surface. The contact angle was extracted from the air/water interface.

of the multilayer and recovers the influence of PSS on the surface properties. In this section, we investigate how these changing surface properties influence the salt rejection of PEM membranes and how the annealing cycles can help as a post-treatment step in regaining control over the membrane surface charge and thus the separation properties. For this study, three types of salts were investigated at a concentration of 5×10^{-3} M: sodium chloride (NaCl), sodium sulfate (Na_2SO_4), and magnesium chloride ($MgCl_2$). Divalent salts were used, in addition to monovalent NaCl, because the PSS/PDADMAC multilayers are known for their high surface charge density and, therefore, the separation of ions is mainly based on Donnan exclusion.[22] To obtain insight into the effect of layer thickness, the membrane separation properties of a 9, 13, and 17 layer thick PEM membrane was studied. The results of the salt retention measurements are shown in **Figure 5**.

In Figure 5A, the retention of the negatively charged divalent sulfate ions across the membrane is plotted for various number of layers. A multilayer with an even number of layers is terminated with PDADMAC and a multilayer with an odd number of layers is terminated with PSS. Here, it can be observed that a multilayer with eight layers, PDADMAC-terminated, has a poor sulfate retention due to its positive surface charge. A multilayer with nine layers, PSS-terminated, has a much higher retention. When the multilayer becomes thicker, forming a 13 and 17 layer thick multilayer, the retention of sulfate ions drops tremendously due to the change in surface charge. This decrease in sulfate ion retention is in line with the observed increase in magnesium ion retention. Magnesium retention is high for PDADMAC-terminated layers and for thicker multilayers (both PDADMAC-terminated and PSS-terminated). In both cases, the multilayers have a positive surface charge which excludes the magnesium ions from the surface and the bulk of the film. For a thin multilayer ended on PSS, magnesium retention is lower due to the almost neutrally charged surface (see Figure 3A).

The effect of annealing on the membrane performance is shown by the dashed columns in Figure 5. Since the PDADMAC/PSS multilayer separates ions on the basis of Donnan exclusion, the effect of annealing (shown in Figure 5A by the dashed columns) on the sulfate retention (Figure 5A) is high for those membranes with 13 and 17 layers. The retention of sulfate ions increased from 38 to 95% after annealing. The sulfate retention of the multilayer with nine layers also substantially improved (94 to 97%, thereby halving sodium sulfate permeation), in agreement with the observed more negative zeta potential (Figure 3B) instead of a neutral zeta potential. These results are also in agreement with the ferricyanide permeability through PSS/PDADMAC multilayers, before and after annealing, in the study of Kelly et al.[39] Since the zeta potential is negative after annealing, the retention of magnesium (shown in Figure 5B) drops greatly for all PSS-terminated multilayers that vary by thickness. For sodium chloride (shown in Figure 5C), the retention for nonannealed membranes is higher when the multilayer is terminated on PDADMAC. This can be explained by the higher surface charge as also shown by the zeta potential measurements, resulting in a stronger exclusion of sodium ions. Interestingly, for the thinnest layer studied (nine layer thick multilayer), the retention increased when the multilayer is annealed. This is in contrast to the other thicknesses where no significant differences were measured. This is expected to be due to the neutral multilayer becoming negatively charged; in this way, the chloride ions are excluded more strongly.

Surprisingly, in Figure 5B a slight increase in the magnesium retention as function of the layer thickness is observed for annealed multilayers. It suggests that the PEM is getting denser, since the sulfate retention does not change as function of the thickness. However, no increase in the sodium chloride retention and no decrease in the permeability is observed. This could be, as described earlier, due to the annealing procedure. The annealing procedure is the same for every PEM membrane. However, when the multilayer is thicker, more PDADMAC is present in the bulk of the multilayer and more annealing cycles are needed to complex all the excess PDADMAC with PSS.[26] Although, in comparison to the previous study, relative thin layers are used in this study. It could be that a thicker multilayer contains more positive charges inside than a thinner layer and that annealing is less successful for thicker multilayers.

All membranes were annealed six times in total. As for the zeta potential measurements, membrane performance was also assessed as function of the number of annealing cycles. In Figure 5D, the sulfate retention is plotted as a function of the number of annealing cycles. Here, the retention does not depend significantly on the number of annealing cycles. This relates to the results obtained from the streaming potential measurements, where the surface charge after the first annealing cycle was the same as after the last annealing cycle. Clearly, one single annealing cycle is sufficient to regain the expected high sulfate retentions.

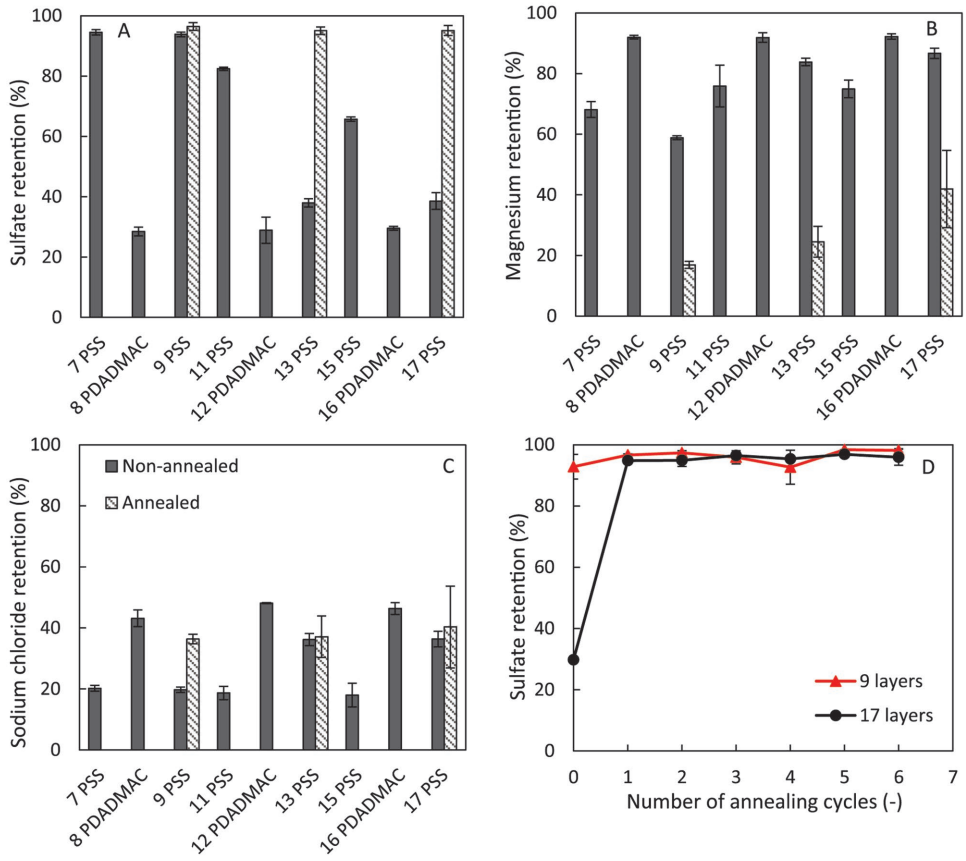

Figure 5. A) Sodium sulfate (Na_2SO_4), B) magnesium chloride ($MgCl_2$), C) sodium chloride (NaCl) retention of PSS/PDADMAC multilayer coated hollow fiber membranes prepared at an ionic strength of 1.0 M of NaCl for various numbers of layers. The solid bars correspond to the retention of the normal PEM-coated membrane. The patterned bars are the retention values for the annealed PEM membranes. All membranes underwent six annealing cycles. D) Sodium sulfate retention as function of the number of annealing cycles.

3. Conclusion

This is the first study to show that PEM post-treatment by salt-annealing can be used to gain control over the surface charge of PEM membranes. In this study, we show that the surface properties of PSS/PDADMAC multilayer membranes become depended on the properties of PDADMAC. For this reason, the surface properties do not dependent anymore on the terminating layer, due to the overcompensation of PDADMAC at thicker layers. The surface charge increases irreversibly to positive values and also contact angles show a high influence of PDADMAC at thicker layers.

It is shown that the change in surface properties has a tremendous effect on the separation properties of the PEM membrane. Sulfate retentions drop from 94 to 39% and magnesium retentions increase from 59% till 87% for PSS-terminated layers, showing that control of the membrane separation properties is lost. Annealing of PSS/PDADMAC multilayers was shown to be effective in order to counteract the overcompensation of PDADMAC and regain control over the membrane separation properties. We show that just a single salt-annealing cycle is enough to regain control over the surface charge of the membrane. For thicker multilayers at which PDADMAC starts to dominate, sulfate retention was increased from 39 to 95% at higher or equal permeability. Even for a multilayer with nine layers, at which PDADMAC is not dominating, salt-annealing can half sulfate permeation (sulfate retention increased from 94 to 97%) in combination with a higher permeability. Clearly, applying salt-annealing as a post-treatment step allows an important additional degree of control over ion permeation. Moreover, the work presented here opens the door to use more annealing approaches to further optimize PEM-membrane performance.

4. Experimental Section

Materials: Polyelectrolytes, poly(diallyldimethylammonium chloride) (PDADMAC, M_w = 200 000–350 000 g mol^{-1}, 20 wt% in water), and poly(sodium 4-styrenesulfonate) (PSS, M_w = 200 000 g mol^{-1}, 30 wt% in water) were purchased from Sigma-Aldrich. Sodium chloride (NaCl) was obtained from Akzo Nobel. Potassium chloride (KCl) was obtained from VWR. All chemicals were used without any further purification.

Hollow fiber membranes were obtained from NX Filtration B.V. (Enschede, the Netherlands) and are based on sulfonated poly(ether sulfone) (SPES) and PDADMAC. The fibers have a positive surface charge, a diameter of 0.68 mm, a standard permeability of 200 L m^{-2} h^{-1} bar^{-1}, and a molecular weight cut-off of 25 kDa. Silicon wafers were purchased from WaferNet Inc. (San Jose, USA).

Polyelectrolyte Multilayer Coating Procedure: Hollow fiber membranes and silicon wafers underwent identical coating treatment, but they were coated separately. Hollow fiber membranes were coated in a bundle. Since the hollow fibers have a positive charge, silicon wafers

were first dipped in a 0.1 g l^{-1} PDADMAC solution at a salt concentration of 1.0 M of NaCl. This was performed to make the comparison between hollow fibers and silicon wafers as equal, therefore, layer zero on silicon wafers is a PDADMAC layer. Subsequently, both hollow fibers and silicon wafers were dipped in a 0.1 g l^{-1} PSS solution at a salt concentration of 1.0 M of NaCl for at least 15 min. After coating the first polyelectrolyte layer, the membranes and wafers were rinsed three times for 5 min in separate rinsing baths containing 1.0 M of NaCl. After rinsing, the next layer was added by immersing the membranes and wafers in a 0.1 g l^{-1} PDADMAC solution at a salt concentration of 1.0 M of NaCl for at least 15 min. After this layer, the membranes and wafers were rinsed in the same fashion as the first layer. This procedure was repeated until the desired number of layers was obtained. Annealing was performed in cycles up to a maximum of 6 cycles, each cycle consist of three sequential steps. The first step is the immersion into a solution containing 2.0 M NaCl for 30 min, followed by the adsorption step in a 0.1 g l^{-1} PSS solution containing 1.0 M of NaCl for 5 min, and ended by a rinsing step with a solution containing 1.0 M of NaCl. After the coating and annealing procedures, the membranes were placed in an aqueous solution containing 15 wt% glycerol for at least 4 h and were subsequently dried overnight. Silicon wafers were blown dry by a stream of nitrogen and stored in a sealed petri dish before measuring.

Contact Angle: Contact angles were measured using the captive bubble method. The captive bubble contact angle was measured on a Dataphysics OCA15 plus. To determine the contact angle a coated silicon wafer was placed coated-side-down in a cell filled with Milli-Q water. Subsequently a 5 µL air bubble was put on the surface of the silicon wafer. To calculate the contact angle a picture was taken five seconds after the air bubble touched the surface of the silicon wafer. Using the SCA20 software the contact angle was calculated. All measurements were performed in threefold and the average values and the standard deviations were calculated and reported.

Ellipsometry: A rotating compensator ellipsometer (Mk-2000 V, J.A. Woollam Co., Inc.) was used for the spectroscopic ellipsometry measurements and was operated in a wavelength range of 370–1000 nm. Samples were measured under three different angles of incidence (65°, 70°, and 75°) and at least three different spots on the silicon wafers were measured. All measurements were done under ambient conditions

$$n(\lambda) = A + \frac{B}{\lambda^2} \tag{1}$$

Data fitting was performed using the CompleteEase software. A standard Cauchy model, shown in Equation (1), was used to fit the data of the polyelectrolyte multilayers. The refractive index of silica and its wavelength dependence is well known and defined. The Cauchy parameters for the polyelectrolyte multilayers were independently fitted from the thickness for layers thicker than 30 nm. Average values with the standard deviations were calculated and reported.

Reflectometry: The growth of a polyelectrolyte multilayer was studied using reflectometry. This technique allows for a quantitative and in situ measurement of the adsorbed amount when polyelectrolytes are coated alternately.[45] A silicon wafer is used in front of a flow cell and the adsorption is measured at the stagnation point. At this stagnation point, the hydrodynamics are well-defined and mass transfer is limited by diffusion. To build the PEM on top of the silicon wafer, polyelectrolyte solutions were alternately flown with rinsing steps in between. At every adsorption step, polyelectrolyte solution was flown long enough to create a stable adsorption value. Polyelectrolyte solutions containing 0.1 g l^{-1} of polyelectrolyte and an ionic strength of 1.0 M NaCl were prepared. Adsorption took place under ambient conditions on a silicon wafer with a layer of 87 nm silicon oxide on top. During the entire experiment the ionic strength was kept constant to ensure a stable signal.

Reflectometry uses monochromatic light of a He-Ne laser (632.8 nm). The light is linearly polarized and is reflected from the wafer at the Brewster angle of 71°. Subsequently, the light is split into its parallel and perpendicular components in the detector. The ratio between the differences in these components relative to the initial state is proportional to the adsorbed amount of mass on the wafer as shown in Equation (2)

$$\Gamma = Q \cdot \frac{\Delta S}{S_0} \tag{2}$$

where Γ is the adsorbed mass in mg m^{-2} on the silicon wafer and S_0 is the initial signal of a bare silicon wafer at the start of the experiment. The sensitivity-factor, also known as the Q-factor, is dependent on the refractive indices (n), thickness of the adsorbed layers (d), angle of incidence (θ), and the refractive index increment (dn/dc) of the multilayers. An optical model was used to calculate the Q-factor of a multilayer made out of PDADMAC and PSS on a silicon wafer that had an 87 nm silicon oxide layer on top. The calculated Q-factor was 25 mg m^{-2} for this case.

Zeta Potential: To determine the zeta potential of the PEM membrane, precoated hollow fiber membranes were placed in modules. Subsequently, the zeta potential was measured using an electrokinetic analyzer (SurPass, Anton Paar, Graz Austria). A 5×10^{-3} M KCl solution was pumped through the hollow fiber module under ambient conditions. The flow of the liquid under a given pressure difference through the hollow fiber module creates a streaming current. Knowing the measured streaming current (A), dI, and the applied pressure difference (Pa), dp, the zeta potential (V), ζ, can be calculated according to Equation (3)

$$\zeta = \frac{dI}{dp} \cdot \frac{\eta}{\varepsilon \cdot \varepsilon_0} \cdot \kappa_B \cdot R \tag{3}$$

where η is the dynamic viscosity (Pa s) of the electrolyte, ε is the dielectric constant (–) of the electrolyte, ε_0 the permittivity of vacuum (F m^{-1}), κ_B the specific electrical conductivity of the electrolyte solution (S m^{-1}), and R is the ohmic resistance (Ω) of the cell measured. Every module was measured six times by the 5×10^{-3} M KCl solution and for every measurement point three membranes were measured. From this data average values and standard errors were derived.

Membrane Performance: To test the membrane performance, single hollow fibers were potted into modules with an effective membrane length of 17 cm. For every type of membrane, three single hollow fiber modules were made and tested in order to obtain average values and standard deviations. Salt retention measurements were performed using NaCl, Na_2SO_4, and $MgCl_2$ to measure the mono- and divalent salt rejection. The measurements were performed in crossflow mode at a transmembrane pressure of 2 bar and a crossflow velocity of 1 m s^{-1}, which corresponds to a Reynolds number of 675 (laminar flow regime). To determine the retention, both the permeate and the feed were measured using a WTW 3210 conductivity meter. Knowing the conductivity of the permeate and the feed, the retention can be calculated by dividing the difference of the conductivities by the feed conductivity, as follows

$$R = \frac{\Delta C}{C_{feed}} \cdot 100\% \tag{4}$$

Acknowledgements

This project was made possible through financial support of Aquaporin A/S (Lyngby, Denmark), and the TKI HTSM, through the University of Twente Impuls program. This project has received funding from the European Research Council (ERC) under the European Union's Horizon 2020 research and innovation programme (ERC StG 714744 SAMBA). The authors would like to thank Joris de Grooth for his useful advice and discussions.

Conflict of Interest

The authors declare no conflict of interest.

Keywords

annealing, ion transport, nanofiltration membranes, polyelectrolyte multilayers

Received: April 28, 2018
Revised: June 28, 2018
Published online: August 6, 2018

[1] M. M. Pendergast, E. M. V. Hoek, *Energy Environ. Sci.* **2011**, *4*, 1946.
[2] R. W. Baker, *Overview of Membrane Science and Technology* in *Membrane Technology and Applications*, John Wiley & Sons, West Sussex, England **2004**, pp. 1–14.
[3] D. Li, H. Wang, *J. Mater. Chem.* **2010**, *20*, 4551
[4] W. J. Lau, A. F. Ismail, N. Misdan, M. A. Kassim, *Desalination* **2012**, *287*, 190.
[5] G. Decher, *Layer-by-Layer Assembly (Putting Molecules to Work)*, in *Multilayer Thin Films: Sequential Assembly of Nanocomposite Materials*, 2nd ed., Vol. *1* (Eds: G. Decher, J. B. Schlenoff), Wiley-VCH, Weinheim, Germany **2012**, pp. 1–21.
[6] G. Decher, *Science* **1997**, *277*, 1232.
[7] P. Lavalle, C. Gergely, F. J. G. Cuisinier, G. Decher, P. Schaaf, J. C. Voegel, C. Picart, *Macromolecules* **2002**, *35*, 4458.
[8] S. T. Dubas, J. B. Schlenoff, *Macromolecules* **1999**, *32*, 8153.
[9] S. S. Shiratori, M. F. Rubner, *Macromolecules* **2000**, *33*, 4213.
[10] J. J. Richardson, M. Bjornmalm, F. Caruso, *Science* **2015**, *348*, 411.
[11] O. Sanyal, I. Lee, *J. Nanosci. Nanotechnol.* **2014**, *14*, 2178.
[12] N. Joseph, P. Ahmadiannamini, R. Hoogenboom, I. F. J. Vankelecom, *Polym. Chem.* **2014**, *5*, 1817.
[13] R. Malaisamy, M. L. Bruening, *Langmuir* **2005**, *21*, 10587.
[14] J. de Grooth, B. Haakmeester, C. Wever, J. Potreck, W. M. de Vos, K. Nijmeijer, *J. Membr. Sci.* **2015**, *489*, 153.
[15] F. Fadhillah, S. M. J. Zaidi, Z. Khan, M. M. Khaled, F. Rahman, P. T. Hammond, *Desalination* **2013**, *318*, 19.
[16] W. Jin, A. Toutianoush, B. Tieke, *Langmuir* **2003**, *19*, 2550.
[17] M. Adusumilli, M. L. Bruening, *Langmuir* **2009**, *25*, 7478.
[18] S. U. Hong, R. Malaisamy, M. L. Bruening, *Langmuir* **2007**, *23*, 1716.
[19] S. U. Hong, R. Malaisamy, M. L. Bruening, *J. Membr. Sci.* **2006**, *283*, 366.
[20] S. U. Hong, O. Y. Lu, M. L. Bruening, *J. Membr. Sci.* **2009**, *327*, 2.
[21] R. A. McAloney, M. Sinyor, V. Dudnik, M. C. Goh, *Langmuir* **2001**, *17*, 6655.
[22] J. de Grooth, R. Oborný, J. Potreck, K. Nijmeijer, W. M. de Vos, *J. Membr. Sci.* **2015**, *475*, 311.
[23] R. A. Ghostine, M. Z. Markarian, J. B. Schlenoff, *J. Am. Chem. Soc.* **2013**, *135*, 7636.
[24] S. B. Abbott, W. M. de Vos, L. L. E. Mears, R. Barker, R. M. Richardson, S. W. Prescott, *Macromolecules* **2014**, *47*, 3263.
[25] R. Kumar, A. F. Ismail, *J. Appl. Polym. Sci.* **2015**, *132*, 42042.
[26] H. M. Fares, Y. E. Ghoussoub, R. L. Surmaitis, J. B. Schlenoff, *Langmuir* **2015**, *31*, 5787.
[27] R. F. Shamoun, H. H. Hariri, R. A. Ghostine, J. B. Schlenoff, *Macromolecules* **2012**, *45*, 9759.
[28] P. A. Patel, A. V. Dobrynin, P. T. Mather, *Langmuir* **2007**, *23*, 12589.
[29] R. Köhler, I. Dönch, P. Ott, A. Laschewsky, A. Fery, R. Krastev, *Langmuir* **2009**, *25*, 11576.
[30] M. Schönhoff, V. Ball, A. R. Bausch, C. Dejugnat, N. Delorme, K. Glinel, R. V. Klitzing, R. Steitz, *Colloids Surf., A* **2007**, *303*, 14.
[31] M. D. Miller, M. L. Bruening, *Chem. Mater.* **2005**, *17*, 5375.
[32] S. Schwarz, K. J. Eichhorn, E. Wischerhoff, A. Laschewsky, *Colloids Surf., A* **1999**, *159*, 491.
[33] G. Ladam, P. Schaad, J. C. Voegel, P. Schaaf, G. Decher, F. Cuisinier, *Langmuir* **2000**, *16*, 1249.
[34] Z. Adamczyk, M. Zembala, P. Warszyński, B. Jachimska, *Langmuir* **2004**, *20*, 10517.
[35] Z. Adamczyk, M. Zembala, M. Kolasińska, P. Warszyński, *Colloids Surf., A* **2007**, *302*, 455.
[36] S. Ilyas, J. de Grooth, K. Nijmeijer, W. M. de Vos, *J. Colloid Interface Sci.* **2015**, *446*, 386.
[37] C. Ringwald, V. Ball, *Colloids Surf., A* **2015**, *464*, 41.
[38] B. Schwarz, M. Schönhoff, *Langmuir* **2002**, *18*, 2964.
[39] K. D. Kelly, H. M. Fares, S. Abou Shaheen, J. B. Schlenoff, *Langmuir* **2018**, *34*, 3874.
[40] C. J. Arias, R. L. Surmaitis, J. B. Schlenoff, *Langmuir* **2016**, *32*, 5412.
[41] H. M. Fares, J. B. Schlenoff, *J. Am. Chem. Soc.* **2017**, *139*, 14656.
[42] R. Malaisamy, A. Talla-Nwafo, K. L. Jones, *Sep. Purif. Technol.* **2011**, *77*, 367.
[43] M. Elzbieciak, M. Kolasinska, P. Warszyński, *Colloids Surf., A* **2008**, *321*, 258.
[44] S. Kostler, A. V. Delgado, V. Ribitsch, *J. Colloid Interface Sci.* **2005**, *286*, 339.
[45] J. C. Dijt, M. A. C. Stuart, G. J. Fleer, *Adv. Colloid Interface Sci.* **1994**, *50*, 79.